Journal of Materials Chemistry B

PAPER

View Article Online
View Journal | View Issue

Cite this: J. Mater. Chem. B, 2014, 2, 4134

Water-soluble bioprobes with aggregation-induced emission characteristics for light-up sensing of heparin†

Ryan T. K. Kwok,‡[ab] Junlong Geng,‡[c] Jacky W. Y. Lam,[ab] Engui Zhao,[ab] Guan Wang,[c] Ruoyu Zhan,[c] Bin Liu*[c] and Ben Zhong Tang*[abd]

Received 5th March 2014
Accepted 22nd April 2014

DOI: 10.1039/c4tb00367e

www.rsc.org/MaterialsB

Two water-soluble cationic fluorene-based fluorescent probes for heparin detection are designed and synthesized. A slight change in the molecular design results in two probes with opposite optical properties in their solution and aggregation states as well as a response to heparin in buffer solution. The probe with a propeller-like conformation exhibits aggregation-induced emission (AIE) characteristics and shows a green fluorescence enhancement upon interaction with heparin; in contrast, the probe with a more planar conformation has a fluorescence quenching response. A comprehensive study on heparin detection using the two probes was conducted, which revealed that the AIE probe shows a better performance than the aggregation-caused quenching (ACQ) probe in terms of sensitivity. The AIE probe integrated with graphene oxide (GO) further improves the heparin detection sensitivity and selectivity. The solution of AIE probe/GO emits strong green fluorescence only in the presence of heparin, which allows for light-up visual discrimination of heparin from its analogues such as chondroitin-4-sulfate and hyaluronic acid. Moreover, the linear light-up response of AIE probe/GO enables heparin quantification in the range of 0–13.2 μM with a detection limit of 10 nM, which is of practical importance for heparin monitoring during surgery or therapy.

Introduction

Heparin, a highly sulfated, negatively charged polysaccharide, plays an important role in the regulation of various physiological processes such as cell growth and differentiation, and inflammatory processes.[1] It has been widely used as an injectable anticoagulant drug to prevent thrombosis during surgery or therapy.[2,3] However, an overdose of heparin could induce catastrophic complications such as hemorrhage or thrombocytopenia.[4–6] Heparin detection and quantification are thus of critical importance. Current clinical laboratory assays for heparin rely on an indirect measurement, which monitors the activated coagulation time or the activated partial thromboplastin time,[7–9] rather than direct measurement of the presence of chemical species. These indirect assays are time-consuming, unreliable and inaccurate because they lack specificity and have potential interference from other factors.[10]

Biosensors based on fluorescent materials have attracted much attention due to their superb sensitivity, selectivity and rapidity. Many cationic materials have been developed for heparin sensing through complexation aided by electrostatic attractions.[11–19] Among which, cationic fluorophores, such as phenylboronic acids,[14] polycationic calyx[8]arenes,[15] and chromophore-tethered flexible copolymers,[16] have been used as heparin receptors. However, the fluorescence emissions of these conventional fluorophores are often partially or completely quenched upon complexation with heparin due to formation of detrimental species such as excimers and exciplexes that generally relax nonradiatively.[20] This aggregation-caused quenching (ACQ) effect has been an intractable obstacle to the development of fluorescent sensors for sensitive quantification of heparin.

Recently, we have discovered that some propeller-like molecules such as tetraphenylethene (TPE) and siloles display a phenomenon that is exactly opposite to the ACQ effect and are non-emissive when molecularly dissolved in solutions but are induced to emit efficiently by aggregate formation.[21–24] We have

[a]HKUST Shenzhen Research Institute, No. 9 Yuexing 1st RD, South Area, Hi-tech Park, Shenzhen, Nanshan, China 518057

[b]Department of Chemistry, Institute for Advanced Study, Division of Biomedical Engineering, Division of Life Science, State Key Laboratory of Molecular Neuroscience and Institute of Molecular Functional Materials, The Hong Kong University of Science and Technology, Clear Water Bay, Kowloon, Hong Kong, China. E-mail: tangbenz@ust.hk

[c]Department of Chemical and Biomolecular Engineering, National University of Singapore, 4 Engineering Drive 4, 117585, Singapore. E-mail: cheliub@nus.edu.sg

[d]Guangdong Innovative Research Team, SCUT-HKUST Joint Research Laboratory, State Key Laboratory of Luminescent Materials and Devices, South China University of Technology, Guangzhou 510640, China

† Electronic supplementary information (ESI) available: Intermediate synthesis; NMR and high resolution mass spectra; size distributions of nanoaggregates; fluorescence photos and emission spectra. See DOI: 10.1039/c4tb00367e

‡ Ryan T. K. Kwok and Junlong Geng contributed equally to this work.

coined this phenomenon as aggregation-induced emission (AIE) and rationalized that the restriction of intramolecular rotations (RIR) in the aggregated state is the main cause for the AIE phenomenon.[25–27] Such a phenomenon is not only of academic value but also of practical implication as it permits the use of dye solutions with any concentration for bioassays and enables the development of "light-up" bioassays by taking advantage of luminogenic aggregation.[21] To date, a variety of AIE luminogens have been prepared and their biological applications in various fields such as cell imaging, and nucleic acids and protein assays have been explored.[28–38] In a previous report, a cationic silole derivative has been utilized for fluorescence "turn-on" sensing of heparin. The probe, however, suffers from strong background noise and non-specific binding to proteins to give false-positive signals.[39] Thus, the development of a "light-up" probe with high sensitivity, selectivity and signal-to-noise ratio for heparin detection is highly appreciated.

Graphene oxide (GO) is a single carbon thin layer decorated with epoxy and hydroxyl groups in its basal planes and carboxyl groups at its periphery. The oxygen-rich functional groups enable GO to interact with biomolecules through covalent, noncovalent or electrostatic interactions. GO is also a well-known fluorescence quencher owing to the strong π–π stacking interactions between GO and organic fluorophores, which induce energy transfer or nonradiative dipole–dipole coupling channels.[40–43] Based on such a unique quenching property, many ultrasensitive GO-based biosensors have been successfully fabricated and applied to detect DNA and proteins.[33,44–50] It, therefore, would be nice if a water-soluble AIE probe could be integrated with GO to develop a sensitive heparin assay.

In this contribution, we report the design and synthesis of a pair of ACQ and AIE water-soluble cationic fluorene-based fluorescent probes for heparin detection. Although the two probes have a similar molecular structure, they display distinctly different optical properties in solution and aggregated states. The probe with a propeller-shaped conformation exhibits AIE characteristic and shows a green fluorescence enhancement upon interaction with heparin; in contrast, the probe with more planar structure shows a fluorescence quenching response. The AIE "light-up" probe enables visual detection of heparin and shows much higher sensitivity than the ACQ "turn-off" probe. With the aid of GO the sensitivity and selectivity of the AIE probe towards heparin are further enhanced. This study highlights the excellent performance of AIE luminophores in bioassays.

Experimental section

Materials

All chemicals and reagents were purchased from Aldrich and used as received without further purification unless otherwise noted. Tetrahydrofuran (THF) was distilled from sodium benzophenone ketyl under nitrogen immediately prior to use. Methanol and ethanol were dried and distilled from calcium oxide. Heparin from bovine intestinal mucosa (Fluka) has 170 U mg^{-1}. The molecular weight of heparin was determined by disaccharide (644.2 g mol^{-1}). Chondroitin 4-sulfate (ChS) from bovine trachea and hyaluronic acid (HA) from *Streptococcus equi* were purchased from BioChemik and used as received. Myoglobin, lysozyme, insulin, cytochrome c and human serum albumin (HSA) were purchased from Aldrich. Graphene oxide (GO) was synthesized from graphite by a modified Hummers method.[51]

Instrumentation

^{1}H and ^{13}C NMR spectra were measured on a Bruker ARX 400 spectrometer in $CDCl_3$ or CD_3OD using tetramethylsilane (TMS; $\delta = 0$) as internal reference. UV spectra were measured on a Biochrom Libra S80PC double beam spectrometer. Photoluminescence spectra (PL) were recorded on a Perkin-Elmer LS 55 spectrofluorometer. High resolution mass spectra (HRMS) were recorded on a GCT premier CAB048 mass spectrometer operating in MALDI-TOF mode. Particle size was determined using a ZetaPlus potential analyzer (Brookhaven instruments corporation, USA).

Synthesis

1,2-Bis[9,9-bis(6-bromohexyl)-2-fluorenyl]-1,2-diphenylethene (1). To a solution of **6** (2.98 g, 5 mmol), zinc dust (0.82 g, 12.5 mmol) in dry distilled THF was added dropwise with titanium(IV) chloride (1.3 mL, 12.5 mmol) under nitrogen at −78 °C. The reaction mixture was warmed to room temperature and then heated to reflux for 12 h. After cooling to room temperature, the reaction was quenched by the addition of hydrochloric acid solution. The mixture was then extracted with dichloromethane several times. The organic layers were combined and washed with saturated brine solution and water, and dried over anhydrous magnesium sulfate. After filtration and solvent evaporation, the product was purified by silica-gel column chromatography using hexane–dichloromethane as eluent to yield **1** as a green oil in 82% yield (2.38 g). ^{1}H NMR (400 MHz, $CDCl_3$), δ (TMS, ppm): 7.61–7.54 (m, 2H), 7.49–7.40 (m, 2H), 7.29–7.22 (m, 6H), 7.13–7.00 (m, 14H), 3.36–3.22 (m, 8H), 1.90–1.49 (m, 16H), 1.26–1.08 (m, 8H), 1.06–0.85 (m, 8H), 0.57–0.43 (m, 8H). ^{13}C NMR (100 MHz, $CDCl_3$), δ (TMS, ppm): 150.5, 149.6, 144.1, 143.3, 140.9, 140.8, 139.3, 131.5, 130.5, 127.6, 126.9, 126.8, 126.4, 126.2, 122.6, 119.6, 118.9, 40.0, 34.0, 32.6, 29.0, 27.8, 23.6. HRMS (MALDI-TOF): m/z 1160.6270 (M^+, calcd 1160.2327).

1,2-Bis{9,9-bis[6-(*N*,*N*,*N*-trimethylammonium)hexyl]-2-fluorenyl}-1,2-diphenylethene tetrabromide (2). To a solution of **1** (25 mg, 0.02 mmol) in THF (5 mL) trimethylamine (2 mL) was added dropwise at −78 °C. The mixture was stirred for 12 h and then allowed to warm to room temperature. The precipitate was redissolved by addition of methanol (5 mL). After the mixture was cooled to −78 °C, additional trimethylamine (2 mL) was added and the mixture was stirred at room temperature for 24 h. After solvent removal, water was added to redissolve all the precipitates and the aqueous solution was extracted with dichloromethane. The aqueous layer was freeze-dried to yield **2** as a greenish powder in 83% yield (25 mg). ^{1}H NMR (400 MHz, CD_3OD), δ (TMS, ppm): 7.69–7.64 (m, 2H), 7.54–7.50 (m, 2H), 7.39–7.34 (m, 2H), 7.33–7.26 (m, 4H), 7.16–6.95 (m, 14H), 3.32–

3.22 (m, 8H), 3.11 (s, 36H), 1.93–1.69 (m, 8H), 1.63–1.52 (m, 8H), 1.16–1.03 (m, 16H), 0.59–0.45 (m, 8H). ^{13}C NMR (100 MHz, CD_3OD), δ (TMS, ppm): 152.1, 151.0, 145.5, 144.7, 142.5, 142.3, 140.9, 132.5, 131.6, 128.9, 128.1, 127.7, 124.2, 121.0, 120.4, 67.6, 60.5, 55.9, 53.7, 41.1, 30.4, 26.9, 23.9. HRMS (MALDI-TOF): *m*/*z* 1317.6105 [$(M - Br)^+$, calcd 1317.6083]. Melting point: 195 °C.

1,2-Bis[9,9-bis(6-bromohexyl)-2-fluorenyl]ethene (3). To a solution of **8** (0.40 g, 0.75 mmol), zinc dust (0.12 g, 1.88 mmol) in dry THF was added dropwise with titanium(IV) chloride (0.2 mL, 1.88 mmol) under nitrogen at −78 °C. The reaction mixture was warmed to room temperature and then heated to reflux for 12 h. After cooling to room temperature, the reaction was terminated by the addition of hydrochloric acid solution. The mixture was then extracted with dichloromethane several times. The organic layers were combined and washed with saturated brine solution and water, and dried over anhydrous magnesium sulfate. After filtration and solvent evaporation, the product was purified by silica–gel column chromatography using hexane–dichloromethane as eluent to yield **3** as a colourless oil in 79% yield (0.30 g). ^{1}H NMR (400 MHz, CDCl3), δ (TMS, ppm): 7.70–7.68 (d, 4H), 7.56–7.52 (m, 4H), 7.36–7.30 (m, 6H), 7.29–7.28 (d, 2H), 3.29–3.24 (t, 8H), 2.03–1.99 (m, 8H), 1.69–1.62 (m, 8H), 1.24–1.16 (m, 8H), 1.12–1.05 (m, 8H), 0.70–0.58 (m, 8H). ^{13}C NMR (100 MHz, $CDCl_3$), δ (TMS, ppm): 150.8, 150.5, 140.8, 136.5, 128.6, 127.1, 126.9, 125.7, 122.7, 120.5, 120.0, 119.7, 54.9, 40.3, 34.0, 32.6, 29.0, 27.7, 23.5. HRMS (MALDI-TOF): *m*/*z* 1008.1726 (M^+, calcd 1008.1701).

1,2-Bis{9,9-bis[6-(*N*,*N*,*N*-trimethylammonium)hexyl]-2-fluorenyl}-ethene tetrabromide (4). To a solution of **3** (50 mg, 0.05 mmol) in THF (10 mL) trimethylamine (4 mL) was added dropwise at −78 °C. The mixture was stirred for 12 h and then allowed to warm to room temperature. The precipitate was redissolved by the addition of methanol (5 mL). After the mixture was cooled to −78 °C, additional trimethylamine (2 mL) was added and the mixture was stirred at room temperature for 24 h. After solvent removal, water was added to redissolve all the precipitate and the aqueous solution was extracted with dichloromethane. The aqueous layer was freeze-dried to yield **4** as a pale yellow powder in 85% yield (53 mg). ^{1}H NMR (400 MHz, CD_3OD), δ (TMS, ppm): 7.76–7.71 (m, 6H), 7.63–7.61 (d, 2H), 7.43–7.39 (m, 4H), 7.36–7.30 (m, 4H), 3.22–3.18 (m, 8H), 3.03 (s, 36H), 2.17–2.10 (m, 8H), 1.59–1.55 (m, 8H), 1.16–1.08 (m, 16H), 0.75–0.52 (m, 8H). ^{13}C NMR (100 MHz, CD_3OD), δ (TMS, ppm): 152.3, 151.9, 142.5, 138.2, 129.7, 128.4, 128.3, 127.0, 124.1, 121.9, 121.1, 120.8, 67.7, 56.3, 53.5, 41.2, 30.2, 26.8, 24.7, 23.6. HRMS (MALDI-TOF): *m*/*z* 1197.8608 [$(M - Br + Cl)^+$, calcd 1196.5187]. Melting point: 202 °C.

Preparation of aggregates

Stock THF solutions of **1** and **3** with a concentration of 1 mM were prepared. An aliquot (0.1 mL) of this stock solution was transferred to a 10 mL volumetric flask. After adding an appropriate amount of THF, water was added dropwise under vigorous stirring to furnish 10 μM THF–water mixtures with water fractions (f_w) of 0–99 vol%. Ethanol and hexane were used to prepare the nanoaggregates of **2** and **4** instead of THF and water. UV, PL and particle size analyses of the resulting mixtures were carried out immediately.

Titration of heparin, ChS and HA

PBS solutions (150 mM, pH = 7.4) of **2** and **4** with a concentration of 12 μM were prepared. Into a cuvette, heparin solution (2 mM) was added dropwise at an interval of 3.3 μL into the PBS solutions of the dye (3 mL). Upon each addition, the mixture was gently mixed using a pipette before the PL measurement. The PL spectra were measured in the wavelength range of 380–700 nm at an excitation wavelength of 365 nm. Titration of ChS and HA was conducted using the same conditions.

Optimization of GO concentration for heparin detection

Into a cuvette, heparin solution (16.5 μL, 2 mM) was added into the PBS solution of **2** (3 mL, 12 μM) to furnish a mixture with a heparin concentration of 11 μM. The GO solution (2.5 mg mL^{-1}) was subsequently added dropwise at an interval of 4.8 μL into the cuvette. The PL spectra were measured in the wavelength range of 380–700 nm at an excitation wavelength of 365 nm. The same experiments were conducted for ChS and HA.

Heparin quantification

A PBS solution of **2** (3 mL, 12 μM) was transferred into cuvettes. Varying concentrations of heparin solutions (0–13.2 μM) were prepared by adding the stock heparin solution (2 mM) at an interval of 3.3 μL. The GO solution (57.6 μL, 2.5 mg mL^{-1}) was subsequently added into the cuvette. The PL spectra were measured from 380–700 nm at an excitation wavelength of 365 nm.

Results and discussion

Design and synthesis

TPE is an archetypal AIE luminophore and emits intense light in the aggregated state despite its solution is almost non-fluorescent. Several fluorescent probes have been developed from TPE-based water-soluble AIE luminogens for sensing of biomacromolecules such as nucleic acids and proteins.[30–32,38] Most of these probes emit blue light. However, for biological applications, it is more desirable to have fluorophores with longer-wavelength emission as they suffer little interference from optical self-absorption and auto-fluorescence from the background. Increasing π-conjugation and introducing donor and acceptor groups in the luminogenic structure are the common ways to red-shift the emission. In this work, the AIE probe **2** has high π-conjugation and hence green emission has been obtained by replacing the two phenyl rings of TPE by fluorene units. Meanwhile, a control probe **4** with stilbene-like structure is also developed by changing the phenyl rings of stilbene into fluorene moieties. The synthetic routes to probes **2** and **4** are depicted in Scheme 1. Compound **5** was synthesized by Friedel–Crafts acylation of fluorene and benzoyl chloride in the presence of $AlCl_3$ as catalyst. It was then coupled with 1,6-dibromohexane in basic solution to afford **6**. Compound **1** was subsequently synthesized by McMurry coupling of **6** catalyzed

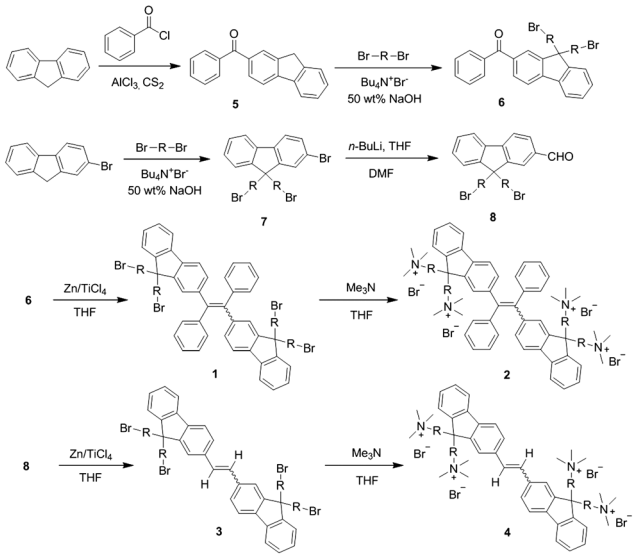

Scheme 1 Synthetic routes to water-soluble cationic fluorene-substituted ethenes **2** and **4**. R = *n*-hexyl.

by $TiCl_4$ and Zn. Treatment of **1** with trimethylamine finally furnished the desirable product **2** in 83% yield. On the other hand, luminogen **4** was synthesized from 2-bromofluorene. Reaction of 2-bromofluorene with 1,6-dibromohexane in the presence of tetrabutylammonium bromide in basic medium gave **7**. Lithiation of **7** with subsequent addition of dimethylforamide afforded formyl fluorene **8**. McMurry coupling of **8** followed by amination with trimethylamine generated **4**. Detailed experimental procedures can be found in the experimental section or ESI.† Flurophores **1–4** were characterized by NMR and MS spectroscopies and gave satisfactory data corresponding to their molecular structures (Fig. S1–8†).

Optical properties

We first studied the optical properties of precursors **1** and **3**. Compounds **1** and **3** are hydrophobic luminogens and dissolve readily in tetrahydrofuran (THF). As shown in Fig. 1A, the UV spectra of **1** in THF solution exhibit two absorption bands at 282 and 348 nm associated with the π–π* transition of the phenyl and fluorene rings, respectively. In contrast, there is only one absorption band recorded at 367 nm in the spectrum of **3**. Although **1** has more π-conjugated units, it shows a blue-shift spectrum, revealing that it adopts a more twisted conformation caused by the steric repulsion between the aryl rings. To verify this assumption, theoretical calculations were carried out. The optimized molecular structures and HOMO and LUMO energy levels of **1** and **3** are shown in Fig. 2. The HOMO and LUMO of **1** are contributed by both orbitals of the phenyl and fluorene rings. Such an X-shaped orbital distribution has somewhat shortened the effective conjugation length. On the other hand, the fluorene rings in **3** lie on the same plane of the vinyl core, thus contributing largely to the energy levels of the luminogen. This orbital distribution results in a linear and extended conjugation in **3**. The calculated energy band gap for **1** is 4.05 eV, which is wider than that of **3** (3.28 eV). Thus, the theoretical study nicely explains the blue-shift in the absorption of **1** from that of **3**.

The photoluminescence (PL) properties of **1** and **3** in the solution and aggregated states are then investigated. In pure THF solution, **1** is non-florescent. The emission remains weak when up to 70% of water is added to the THF solution (Fig. 3). Afterwards, the PL starts to increase swiftly. The higher the water fraction, the stronger is the light emission. At 90% water content, the PL intensity at 502 nm is 120-fold higher than that in pure THF solution. The fluorescence enhancement of **1** is attributed to the formation of nano-aggregates as suggested by the particle size analysis (Fig. S9†). Clearly, **1** is AIE-active. In contrast, **3** displays an opposite luminescence behaviour. In pure THF solution, **3** fluoresces strongly at 420 nm. Addition of water into the THF solution, however, has quenched the light emission progressively. At 99% aqueous mixture, only a very weak signal is recorded, suggesting that **3** is a typical ACQ luminogen. The fluorescence photos of THF–water mixtures of **1** and **3** with different water fractions taken under UV illumination also demonstrate the distinct opposite PL properties of **1** from that of **3** (Fig. S10†).

After investigating the PL of the precursors **1** and **3**, we further examined the optical properties of **2** and **4** to see whether amination would affect the light emission process. Due to their cationic character, **2** and **4** are soluble in water and

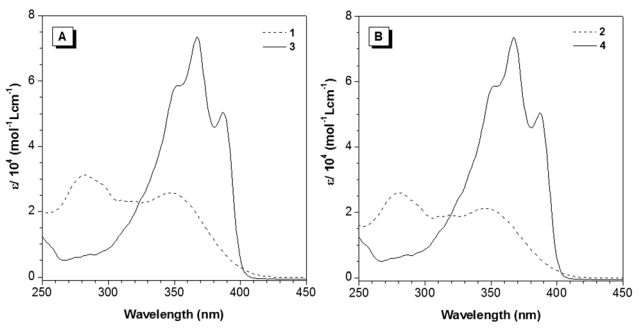

Fig. 1 UV spectra of (A) **1** and **3** in THF and (B) **2** and **4** in ethanol. Concentration: 10 μM.

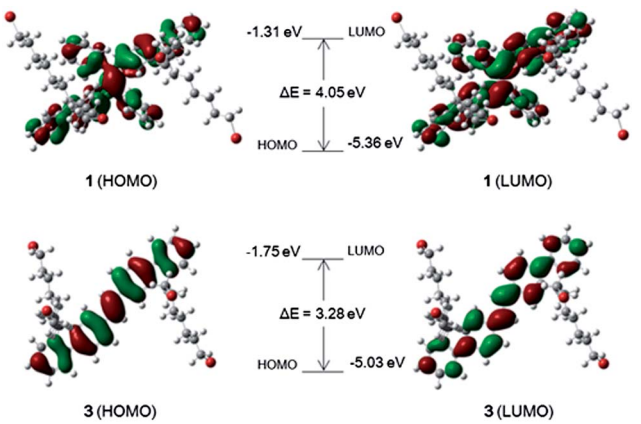

Fig. 2 Molecular amplitude plots HOMO and LUMO of **1** and **3**.

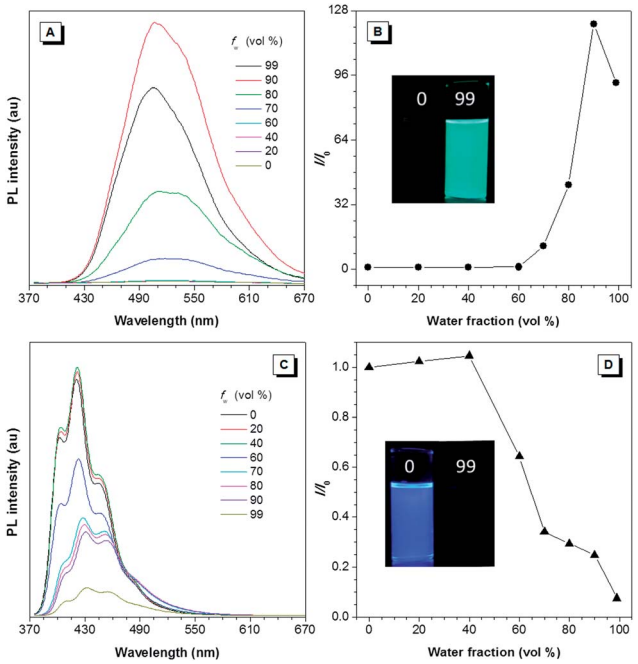

Fig. 3 PL spectra of (A) **1** and (C) **3** in THF–water mixtures with different water fractions (f_w). Concentration: 10 μM; excitation wavelength: 365 nm. (B and D) Plots of relative PL intensity (I/I_0) of (B) **1** at 502 nm and (D) **3** at 420 nm *versus* the composition of THF–water mixtures of **1** and **3**. I_0 = PL intensity in pure THF solution ($f_w = 0$). Inset: fluorescence photos of THF–water mixtures of (upper) **1** and (lower) **3** at f_w = 0 and 99 vol% taken under 365 nm UV illumination from a hand-held UV lamp.

ethanol but insoluble in hexane. Thus, ethanol or PBS buffer and ethanol–hexane mixture are chosen for the UV measurement and PL analysis in the solution and aggregated state, respectively. The UV spectra of **2** and **4** in ethanol (Fig. 1B) and in PBS buffer (Fig. S11†) resemble those of the precursors **1** and **3** in THF. While **2** absorbs at 280 and 350 nm, the absorption maximum of **4** occurs at a longer wavelength of 368 nm, which is in correlation with the fact that its precursor **3** is more conjugated than **1**. Similar to **1**, **3** is AIE-active: its ethanol solution gives almost no light upon photoexcitation but its nano-aggregates in the ethanol–hexane mixture with 80% hexane content are strong green emitters (Fig. S12–S13†). Luminogen **4** inherits the ACQ characteristics from **3**. While it emits intense blue light in ethanol but it becomes non-emissive when its molecules aggregate in the ethanol–hexane mixture with 99% hexane content. Visual observation of the fluorescence photos of **2** and **4** in the ethanol–hexane mixtures with different hexane fractions also demonstrates the AIE and ACQ features of **2** and **4**, respectively (Fig. S14†). These results indicate that the amination reaction only enhances the water solubility of the fluorophores but exerts no effect on their optical properties.

Heparin detection

The obvious difference in emission behaviours of **2** and **4** promotes us to compare their sensing performance in heparin detection and differentiation of its analogues such as chondroitin-4-sulfate (ChS) and hyaluronic acid (HA) (Scheme 2), which often exist as contaminants in heparin samples.

The principle of fluorescence assay of heparin and its analogues using **2** and **4** is illustrated in Scheme 3. Addition of negatively-charged analytes induces the formation of the probe-analyte complex through electrostatic interactions, which triggers fluorescence change. Due to the different affinity of the analytes to the dye molecules, different extents of PL changes are expected.

Titration of **2** and **4** with heparin and its analogues (0–11 μM) was conducted in PBS buffer (150 mM, pH = 7.4) and the corresponding PL spectra are shown in Fig. 4 and Fig. S15–16.† Luminogen **2** shows a slight stronger PL in PBS buffer than in water, presumably due to the slight aggregation of the fluorophore in this aqueous medium. The emission becomes stronger gradually when an increasing amount of heparin is added to the buffer solution. The complexation of **2** with heparin has activated the RIR process of the fluorophore, which reduces the energy loss *via* nonradiative relaxation channels and hence turns on the PL of **2**. In the presence of 11 μM of heparin, the PL intensity increases by ~3-fold. Such a "light-up" phenomenon was also observed when ChS, instead of heparin, was used but the maximum emission enhancement was merely 1.4-fold. The lower charge density of ChS compared to heparin maybe the major reason to account for the smaller magnitude of fluorescence enhancement. The PL of **2** changes little in the presence of HA, which is indicative of no or very weak electrostatic interactions between **2** and HA. On the other hand, since **4** is an ACQ dye, it is highly emissive in PBS buffer. Addition of 11 μM of heparin and ChS, respectively, to the buffer solution, has quenched the light emission by 50 and 80%. Similar to **2**, HA causes no observable change on the PL of **4**. Such results show that the AIE probe **2** has a higher sensitivity than the ACQ probe

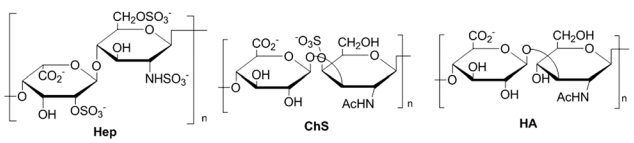

Scheme 2 Chemical structures of heparin (Hep), chondroitin 4-sulfate (ChS) and hyaluronic acid (HA).

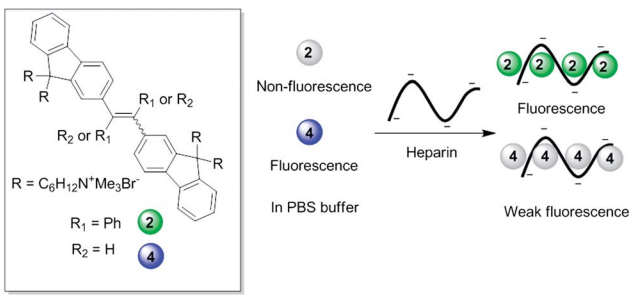

Scheme 3 Schematic illustration of detection of heparin and its analogues by **2** and **4** in PBS buffer.

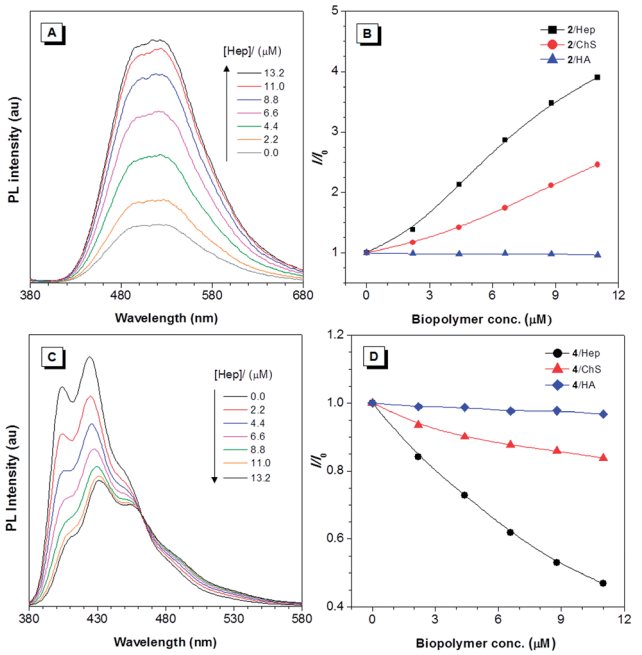

Fig. 4 Titration of (A) **2** and (C) **4** with different concentrations of heparin in PBS buffer (150 mM, pH = 7.4). Dye concentration: 12 μM; excitation wavelength: 365 nm. (B and D) Plots of relative PL intensity (I/I_0) of (B) **2** at 520 nm and (D) **4** at 424 nm *versus* Hep, ChS or HA concentrations in PBS buffer.

4 in heparin detection. However, selectivity still needs to be improved in order to discriminate heparin from ChS.

Dye/GO complex for heparin sensing

To further improve the sensitivity and selectivity of the AIE probe **2** in heparin sensing, GO is introduced into the assay system. The schematic illustration of the fluorescence assay for heparin using **2** integrated with GO is shown in Scheme 4.

Addition of GO into the buffer solution of the **2**/analyte complex may disassemble the complex due to the competition of GO with the analyte for **2**, the extent of which depends on the charge density of the analyte. For analytes such as ChS and HA with low charge density, GO wins the competition. This disassembles the dye/biopolymer complex and subsequently weakens the light emission. In contrast, heparin is highly negatively-charged and thus shows stronger affinity to bind with **2** than GO. With such regard, the strong fluorescence from the **2**/Hep complex can be preserved. To prove such speculation, we first introduced GO into **2** in PBS buffer. The intrinsic fluorescence of **2** in PBS buffer (12 μM) becomes weaker upon addition of GO and is quenched completely at a concentration of 10 μg mL^{-1} GO. This implies the strong binding of **2** to GO and GO is really an efficient PL quencher. The fluorescence change of buffer solutions of dye/biopolymer complexes upon addition of different concentrations of GO are then studied (Fig. 5A). With an increase in the GO concentration, the emission from all the solutions decreased gradually. However, the decay rate for the **2**/Hep solution is much slower than those for **2**/ChS and **2**/HA solutions, thanks to the tight complex formed by **2** and heparin. The largest emission difference between **2**/Hep/GO, **2**/ChS/GO and **2**/HA/GO is found at [GO] = 48 μg mL^{-1}, which is most likely to be the optimum GO concentration for the heparin quantification study. Indeed, as shown in Fig. 5B, the PL of **2**/Hep/GO is 13 and 146-fold higher than those of **2**/ChS/GO and **2**/HA/GO, respectively at 520 nm. To further address the selectivity of the **2**/GO system towards heparin, a control experiment with other proteins including myoglobin, lysozyme, insulin, cytochrome c, and human serum albumin (HSA) is performed under the same experimental conditions. As shown in Fig. S17,† only the fluorescence of the **2**/Hep complex is preserved in the presence of GO. While in the case of other protein complexes with **2**, most of the fluorescence are quenched once GO is introduced. Obviously, introducing GO into **2** in the heparin assay has greatly improved the assay sensitivity and selectivity.

Heparin quantification

Heparin quantification is conducted in PBS buffer (150 mM, pH = 7.4) with an optimum dye GO concentration of 12 μM and 48 μg mL^{-1}, respectively. While, no fluorescence is detected when **2** is integrated with GO, the buffer solution starts to emit when heparin is added (Fig. 6A). The plot of $(I/I_0 - 1)$ *versus* the heparin concentration gives a linear curve in the range of 0–13.2 μM (Fig. 6B). Such a detection range is suitable for heparin

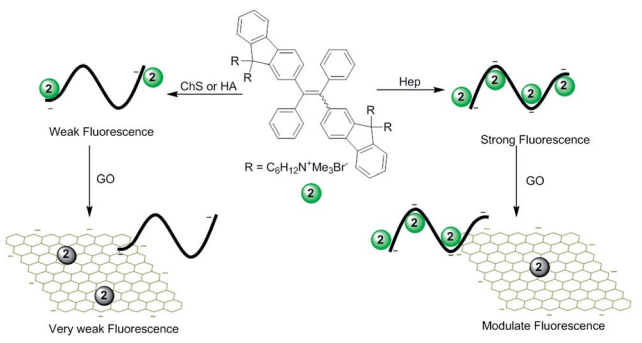

Scheme 4 Schematic illustration of heparin and its analogues detection with **1**/GO.

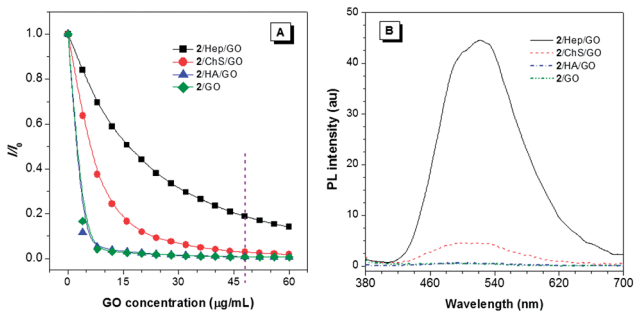

Fig. 5 (A) Change in the relative PL intensity (I/I_0) of **2**/Hep, **2**/ChS or **2**/HA in PBS buffer with GO concentration, where I and I_0 are the PL intensity of **2**/Hep, **2**/ChS or **2**/HA at 520 nm in the presence or absence of GO, respectively. (B) PL spectra of **2**/Hep, **2**/ChS, **2**/HA and **2** with 48 μg mL^{-1} GO in PBS buffer. Concentration (μM): 12 (**2**) and 11 (Hep, ChS or HA); excitation wavelength: 365 nm.

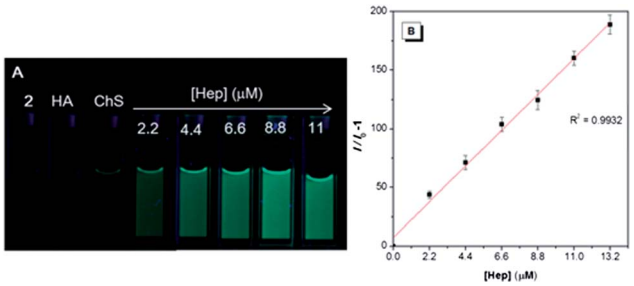

Fig. 6 (A) Fluorescence photos of **2**/GO in PBS buffer in the absence and presence of HA, ChS or Hep taken under 365 nm UV illumination using a hand-held UV lamp. Concentration: 12 μM (**2**), 11 μM (HA and ChS), 2.2–11 μM (Hep), 48 μg mL^{-1} (GO). (B) Calibration curve for Hep quantitation. Concentration: 12 μM (**2**); 48 μg mL^{-1} (GO); excitation wavelength: 365 nm.

monitoring during surgery or therapy (2–11 μM).[50] The lower detection limit for the heparin assay is determined to be 10 nM, based on $3 \times S_0/S$, where S_0 is the standard deviation of background and S is the sensitivity.

Conclusions

Two cationic fluorene-based fluorescent probes have been synthesized for heparin detection. The AIE probe performs better than the ACQ probe in terms of sensitivity and selectivity. The AIE probe integrated with GO enables "light-up" heparin quantification in a concentration range of 0–13.2 μM with a detection limit of 10 nM, which is of practical use for heparin monitoring during surgery or therapy. This study not only provides an assay for rapid quantification of heparin, but also demonstrates that the water-soluble AIE luminogens are promising biosensors by taking advantage of the strong fluorescence of its complexes with biomacromolecules.

Acknowledgements

This work was partially supported by the National Basic Research Program of China (973 Program; 2013CB834701), the Research Grants Council of Hong Kong (604711, 604913, HKUST2/CRF/10 and N_HKUST620/11), Innovation and Technology Commission (ITCPD/17-9), the University Grants Committee of Hong Kong (AoE/P-03/08) and the Singapore Ministry of Defense (R279-000-340-232). B. Z. T. is grateful for the support from the Guangdong Innovative Research Team Program of China (201101C0105067115).

Notes and references

1 I. Capila and R. J. Linhardt, *Angew. Chem., Int. Ed.*, 2002, **41**, 391–412.
2 J. Fareed, D. A. Hoppensteadt and R. L. Bick, *Semin. Thromb. Hemostasis*, 2000, **26**, 5–21.
3 R. J. Linhardt and N. S. Gunay, *Semin. Thromb. Hemostasis*, 1999, **25**, 5–16.
4 T. E. Warkentin, M. N. Levine, J. Hirsh, P. Horsewood, R. S. Roberts, M. Gent and J. G. Kelton, *N. Engl. J. Med.*, 1995, **332**, 1330–1335.
5 B. Girolami and A. Girolami, *Semin. Thromb. Hemostasis*, 2006, **32**, 803–809.
6 G. J. Despotis, G. Gravlee, K. Filos and J. Levy, *Anesthesiology*, 1999, 1122–1151.
7 P. D. Raymond, M. J. Ray, S. N. Callen and N. A. Marsh, *Perfusion*, 2003, 269–277.
8 D. J. Murray, W. J. Brosnahan, B. Pennell, D. Kapalanski, J. M. Weiler and J. Olson, *J. Cardiothor. Vasc. An.*, 1997, **11**, 24–28.
9 B. Boneul and P. de Moerloose, *Semin. Thromb. Hemostasis*, 2001, **27**, 519–522.
10 M. N. Levine, J. Hirsh, M. Gent, A. G. Turpie, M. Cruickshank, J. Weitz, D. Anderson and D. Johnson, *Arch. Intern. Med.*, 1994, **154**, 49–56.
11 K.-Y. Pu and B. Liu, *Adv. Funct. Mater.*, 2009, **19**, 277–284.
12 R. Zhan, Z. Fang and B. Liu, *Anal. Chem.*, 2010, **82**, 1326–1333.
13 E. Climent, P. Calero, M. D. Marcos, R. Martínez-Máñez, F. Sancenón and J. Soto, *Chem.–Eur. J.*, 2009, **15**, 1816–1820.
14 A. T. Wright, Z. Zhong and E. V Anslyn, *Angew. Chem., Int. Ed.*, 2005, **44**, 5679–5682.
15 T. Mecca, G. M. L. Consoli, C. Geraci, R. La Spina and F. Cunsolo, *Org. Biomol. Chem.*, 2006, **4**, 3763–3768.
16 W. Sun, H. Bandmann and T. Schrader, *Chem.–Eur. J.*, 2007, **13**, 7701–7707.
17 J. C. Sauceda, R. M. Duke and M. Nitz, *ChemBioChem*, 2007, **8**, 391–394.
18 R. B. C. Jagt, R. F. Gómez-Biagi and M. Nitz, *Angew. Chem., Int. Ed.*, 2009, **48**, 1995–1997.
19 R. S. Dey and C. R. Raj, *Chem.–Asian J.*, 2012, **7**, 417–424.
20 J. B. Birks, *Photophysics of Aromatic Molecules*, Wiley, London, New York, 1970.
21 Y. Hong, J. W. Y. Lam and B. Z. Tang, *Chem. Commun.*, 2009, 4332–4353.
22 M. Wang, G. Zhang, D. Zhang, D. Zhu and B. Z. Tang, *J. Mater. Chem.*, 2010, **20**, 1858.
23 Y. Hong, J. W. Y. Lam and B. Z. Tang, *Chem. Soc. Rev.*, 2011, **40**, 5361–5388.
24 J. Luo, Z. Xie, J. W. Y. Lam, L. Cheng, B. Z. Tang, H. Chen, C. Qiu, H. S. Kwok, X. Zhan, Y. Liu and D. Zhu, *Chem. Commun.*, 2001, **381**, 1740–1741.
25 J. Chen, C. C. W. Law, J. W. Y. Lam, Y. Dong, S. M. F. Lo, I. D. Williams, D. Zhu and B. Z. Tang, *Chem. Mater.*, 2003, **79**, 1535–1546.
26 Z. Li, Y. Dong, B. Mi, Y. Tang, M. Häussler, H. Tong, Y. Dong, J. W. Y. Lam, Y. Ren, H. H. Y. Sung, K. S. Wong, P. Gao, I. D. Williams, H. S. Kwok and B. Z. Tang, *J. Phys. Chem. B*, 2005, **109**, 10061–10066.
27 Z. Zhao, Z. Wang, P. Lu, C. Y. K. Chan, D. Liu, J. W. Y. Lam, H. H. Y. Sung, I. D. Williams, Y. Ma and B. Z. Tang, *Angew. Chem., Int. Ed.*, 2009, **48**, 7608–7611.
28 C. W. T. Leung, Y. Hong, S. Chen, E. Zhao, J. W. Y. Lam and B. Z. Tang, *J. Am. Chem. Soc.*, 2013, **135**, 62–65.

29 W. Qin, D. Ding, J. Liu, W. Z. Yuan, Y. Hu, B. Liu and B. Z. Tang, *Adv. Funct. Mater.*, 2012, **22**, 771–779.
30 Y. Hong, H. Xiong, J. W. Y. Lam, M. Häussler, J. Liu, Y. Yu, Y. Zhong, H. H. Y. Sung, I. D. Williams, K. S. Wong and B. Z. Tang, *Chem.–Eur. J.*, 2010, **16**, 1232–1245.
31 Y. Hong, L. Meng, S. Chen, C. W. T. Leung, L.-T. Da, M. Faisal, D.-A. Silva, J. Liu, J. W. Y. Lam, X. Huang and B. Z. Tang, *J. Am. Chem. Soc.*, 2012, **134**, 1680–1689.
32 H. Shi, R. T. K. Kwok, J. Liu, B. Xing, B. Z. Tang and B. Liu, *J. Am. Chem. Soc.*, 2012, **134**, 17972–17981.
33 X. Xu, J. Li, Q. Li, J. Huang, Y. Dong, Y. Hong, J. Yan, J. Qin, Z. Li and B. Z. Tang, *Chem.–Eur. J.*, 2012, **18**, 7278–7286.
34 M. Nakamura, T. Sanji and M. Tanaka, *Chem.–Eur. J.*, 2011, **17**, 5344–5349.
35 T. Noguchi, T. Shiraki, A. Dawn, Y. Tsuchiya, L. T. N. Lien, T. Yamamoto and S. Shinkai, *Chem. Commun.*, 2012, **48**, 8090–8092.
36 X. Wang, A. R. Morales, T. Urakami, L. Zhang, M. V Bondar, M. Komatsu and K. D. Belfield, *Bioconjugate Chem.*, 2011, **22**, 1438–1450.
37 D. A. Links, *J. Mater. Chem.*, 2011, 3170–3177.
38 M. Wang, D. Zhang, G. Zhang, Y. Tang, S. Wang and D. Zhu, *Anal. Chem.*, 2008, **80**, 6443–6448.
39 M. Wang, D. Zhang, G. Zhang and D. Zhu, *Chem. Commun.*, 2008, 4469–4471.
40 X. Qi, H. Li, J. W. Y. Lam, X. Yuan, J. Wei, B. Z. Tang and H. Zhang, *Adv. Mater.*, 2012, **24**, 4191–4195.
41 L. Cai, R. Zhan, K. Pu, X. Qi, H. Zhang, W. Huang and B. Liu, *Anal. Chem.*, 2011, 7849–7855.
42 X. Huang, X. Qi, F. Boey and H. Zhang, *Chem. Soc. Rev.*, 2012, **41**, 666–686.
43 X. Gu, G. Yang, G. Zhang, D. Zhang and D. Zhu, *ACS Appl. Mater. Interfaces*, 2011, **3**, 1175–1179.
44 C.-H. Lu, J. Li, J.-J. Liu, H.-H. Yang, X. Chen and G.-N. Chen, *Chem.–Eur. J.*, 2010, **16**, 4889–4894.
45 F. Liu, J. Y. Choi and T. S. Seo, *Biosens. Bioelectron.*, 2010, **25**, 2361–2365.
46 H. Dong, W. Gao, F. Yan, H. Ji and H. Ju, *Anal. Chem.*, 2010, **82**, 5511–5517.
47 S. He, B. Song, D. Li, C. Zhu, W. Qi, Y. Wen, L. Wang, S. Song, H. Fang and C. Fan, *Adv. Funct. Mater.*, 2010, **20**, 453–459.
48 Y. Wang, Z. Li, J. Wang, J. Li and Y. Lin, *Trends Biotechnol.*, 2011, **29**, 205–212.
49 X. Xu, J. Huang, J. Li, J. Yan and Z. Li, *Chem. Commun.*, 2011, 12385–12387.
50 D. L. Rabenstein, *Nat. Prod. Rep.*, 2002, **19**, 312–331.
51 Y. Xu, H. Bai, G. Lu, C. Li and G. Shi, *J. Am. Chem. Soc.*, 2008, **130**, 5856–5857.